Published Online on 13 October 2015

Proc Indian Natn Sci Acad **81** No. 4 September 2015 pp. 787-800

DOI: 10.16943/ptinsa/2015/v81i4/48297

Review Article

Hydrate Reservoirs – Methane Recovery and CO_2 Disposal

K MURALIDHAR* and MALAY K DAS

Department of Mechanical Engineering, Indian Institute of Technology Kanpur, Kanpur 208 016, India

(Received on 02 March 2014; Accepted on 02 August 2015)

The world over, energy generation technologies such as gas turbines and fuel cells have initiated a migration towards gaseous fuels. A driving force for this trend is the C:H ratio, with the hydrogen component progressively increasing with time. In the ultimate analysis, it suggests a migration towards hydrogen. Meanwhile, the search for viable hydrocarbons continues since their combustion and utilization characteristics are understood. Gas reservoirs of limited significance have been found within the country, for example, coal bed methane and shale gas. Additionally, the prospect of obtaining gas in the long run, from gas hydrate reservoirs may become a reality. Such reservoirs have an added potential of storing large quantities of CO_2 in hydrate form. Consequently, technologies from extraction of gas hydrates, energy conversion to an appropriate form all the way to exhaust gas disposal need to be re-visited and developed in the local context. As a start, this study describes a mathematical model of multi-species multi-phase transport in a porous reservoir, based on principles of conservation of mass, momentum and energy. The model equations are discretized and numerically solved to simulate flow and heat transfer in the hydrate reservoir, bounded by a depressurization and an injection well. As seen in the simulation, depressurization extracts methane from the reservoir while CO_2 injection enhances the recovery rate largely due to the displacement of CH_4 by CO_2. At the same time, hydrate formation of CO_2 traps it in the reservoir providing additional structural integrity to the marine geological formation. The model, validated on a laboratory scale, needs to be tested under field-scale conditions.

Keywords: Gas Hydrates; Methane Recovery; CO_2 Disposal; Mathematical Modelling; Depressurization Technique

What Are Gas Hydrates?

Gas hydrates refer to a class of solid crystalline compounds where guest gas molecules are caged in a solid H_2O lattice (Sloan and Koh, 2007). Among commonly occurring gas hydrates, methane hydrate, present in the marine sediments, is now identified as a potential source of hydrocarbon fuel (Fig. 1). The global storage of methane in the hydrate form exceeds all other known hydrocarbon reserves. Extraction of methane from marine sediments however, poses multiple challenges and opportunities to the practising engineer. Safe extraction processes that keep the fragile marine-ecosystem unaltered require significant infrastructural investment. On the other hand, methane extraction from the gas hydrate provides an option for CO_2 sequestration. Furthermore, controlled extraction impedes the possibility of accidental release of methane due to global warming. It may be mentioned that uncontrolled release of methane, a potent greenhouse gas, may seriously endanger the global ecosystem. It is, therefore, imperative to examine and identify the possible technologies for methane extraction from marine sediments. Among the possible techniques, depressurization, and injection have been identified as the two most promising ways for extracting methane from the gas hydrate stored in the marine sediments; a model arrangement for depressurization is shown in Fig. 2.

Depressurization requires destabilizing the chemical structure of the gas hydrate by lowering the pressure below the thermodynamic limit. Since the gas hydrate is stable only at high-pressure (~10 MPa)

**Author for Correspondence: E-mail: kmurli@iitk.ac.in; Mob.: 9919373363; Tel.: 0512 2597182*

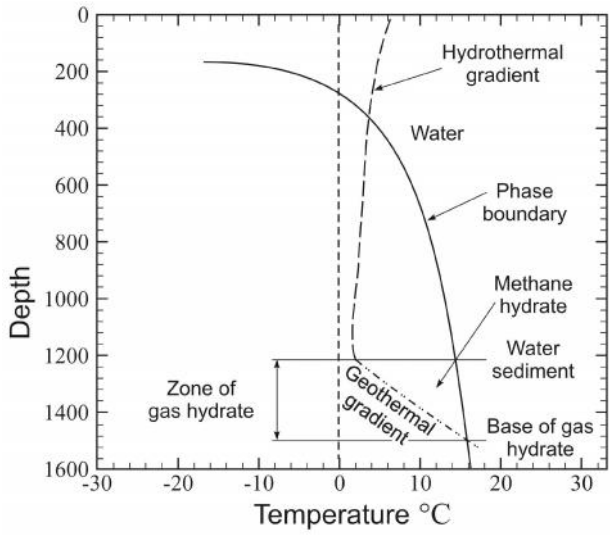

Fig. 1: Representative diagram indicating the occurrence of gas hydrates at the ocean floor; depth in metres

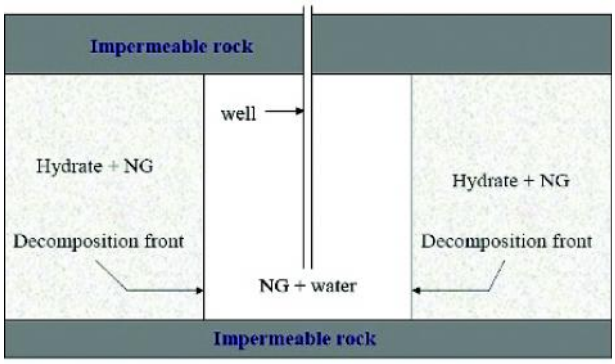

Fig. 2: A possible configuration for depressurization a gas hydrate reservoir. NG stands for natural (free) gas. In the schematic, the decomposition front moves outwards from the central well while gas released from the formation moves inwards towards the well

and below ambient temperature environment, depressurization seems to be a suitable approach for methane extraction. Such a process also guarantees controlled release of methane by precisely adjusting the extraction pressure. In contrast to depressurization, the injection processes attempt to replace the methane encaged in the hydrate-lattice with another suitable gas. Both processes have their advantages and disadvantages. While depressurization facilitates rapid release of CH_4, the process may weaken the hydrate-bearing structure. Injection, on the other hand, ensures structural stability at the expense of being slow and energy-intensive. Additionally, the injecting gas needs to be non-corrosive in nature and should have lower free energy than methane at the hydrate-formation environment. Recent research suggests that CO_2 may serve as a suitable injection species for hydrate extraction (White *et al.*, 2011). In undersea environment, CO_2 may form stable hydrates replacing and thus releasing CH_4. While such a process ensures structural stability of the hydrate-bearing sediments, the effect of the acidic nature of CO_2 has to be carefully investigated. Also important is to understand the role of water salinity on the overall process dynamics. It is now agreed that no single process may be suitable for all types of hydrate reservoirs. Emerging trends include the development of hybrid processes to combine the flexibilities of both depressurization and injection for the safe extraction of CH_4 at a reasonable rate.

Apart from recovering methane, the importance of gas hydrates is immense. Among other possibilities, gas hydrate reservoirs can additionally act as a sink for natural gas apart from being a cold thermal energy storage unit. The storage capacity in the form of hydrates is considerable. For natural gas, it yields a benefit of approximately 150 times the storage capacity of compressed gas. The large storage potential of gas hydrates makes it attractive for storing and transportation of natural gas, being an alternative to liquefaction and compression.

Background

Exploration of gas hydrates was initiated in 1996 by the Gas Authority of India Limited of the Ministry of Petroleum & Natural Gas. The National Gas Hydrate Programme (NGHP) created under the Directorate General of Hydrocarbons (DGH) has attracted participation from public sector organizations such as ONGC, OIL and GAIL, and CSIR laboratories such as NGRI and NIO. Their studies have established the presence of gas hydrates under the ocean bed of the Indian peninsula (Sain and Gupta, 2012). Significant amount of free gas has been detected below the hydrate-rich formation. The estimated quantity is large enough to support the energy security of the country for the next 100 years. Gas hydrates reserves have been located at the Krishna-Godavari,

Mahanadi, Andaman, Kerala-Konkan, and Saurashtra regions at water depths of 500 to 2500 m.In general terms, gas hydrates, essentially a methane source, have been located around the world in significantly large quantities. Thus, the availability of a new energy source can be taken to be practically proven. The next step is to work out technologies of mining the energy-bearing material in a stable and cost-effective manner, and create devices to convert the available chemical energy into useful work. Related questions of environmental impact and management are significant points of concern.

Technology development for the utilization of gas hydrates calls for an intensive, yet coordinated and multi-disciplinary research. It requires an understanding of natural phenomena on one hand, and development and design of engineering systems on the other. Issues to be addressed include physico-chemical hydrodynamics of flow of methane in natural formations, energy exchanges with the host rock, chemical reactions and changes in the structural integrity of the host formation. The gas thus recovered from a site can be liquefied and transported to gas turbine installations for power generation. Alternatively, power can be generated locally using newer technologies such as fuel cells. Many of these decisions will depend on economic factors, but the need to anticipate all possible scenarios cannot be over-emphasized. In the last few years, government agencies in USA, Canada, Russia, Japan and South Korea have begun to develop hydrate research programmes to recover gas from oceanic hydrates.

The volume of CO_2 emissions from methane utilization has been estimated to be quite large. From an environmental viewpoint (specifically, global warming), it would violate international agreements, such as the Kyoto protocol and a remedial action would be called for. A suggestion being vigorously pursued internationally is the process of carbon sequestration, wherein the products of combustion (essentially CO_2) are pumped back into the gas hydrates formation (Ota *et al*., 2005). In recent proposals, CO_2 is liquefied before being disposed into hydrate reservoirs. The presence of CO_2 in place of CH_4 has the added advantage of providing structural support to the reservoir. The technological feasibility of such an idea is yet to be fully ascertained.

Forward modelling of chemical instability and gas recovery from hydrates, generation of phase equilibrium diagrams, and performance evaluation of engineering configurations have just commenced. The connection between laboratory-scale measurements and field scale performance, called *scale-up*, is established against the background of a mathematical model. Related tasks are parameter estimation and data retrieval from field measurements. It calls for wide ranging experiments on gas recovery, power generation, and management of the environment.

Methane Recovery

Methane can be recovered from gas hydrates by modifying the chemical equilibrium conditions in the reservoir (Fig. 3). Three methods proposed are depressurization, inhibitor injection and thermal stimulation. Cost considerations as well as environmental protection dictate the choice of the recovery method. In the depressurization technique, the reservoir pressure is reduced below the three-phase equilibrium curve. The composite hydrate molecule containing H_2O and CH_4 dissociates by

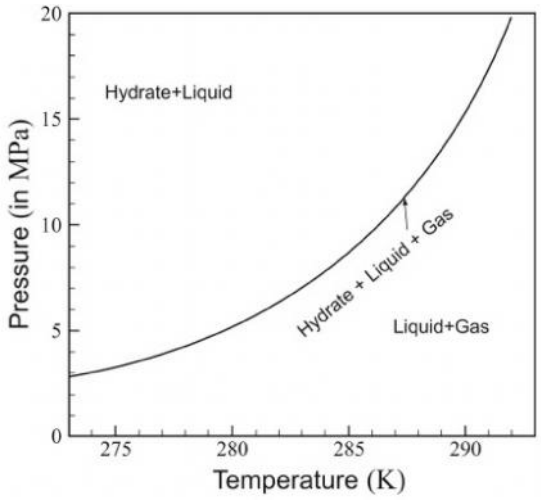

Fig. 3: Phase equilibrium line that shows the stability boundary on the pressure-temperature plane. The region below the solid line indicates gas separated from the water cage. In the region above the line, gas hydrates are stable and methane is trapped in a cage of water molecule

absorbing thermal energy from its surroundings. This step leads to a reduction in the reservoir temperature. Locally, a new equilibrium condition is achieved at a lower pressure and lower temperature but a certain amount of gas is released.

In the inhibitor injection technique, chemicals that shift the stability curve upwards are made use of. Accordingly, on injection of the chemical into the gas hydrate bed, dissociation of methane from hydrate will occur (Fig. 4). In the natural gas industry, alcohols

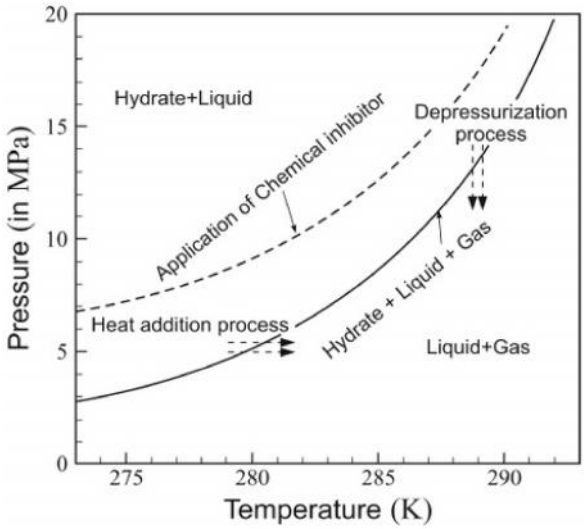

Fig. 4: Schematic drawing of the effect of chemical inhibitor on the stability curve. The movement of the stability boundary upwards shows that gas release is possible under a broader set of pressures and temperatures

(methanol) and glycols have been proposed to inhibit hydrate formation and are thus suitable for forcing dissociation of gas hydrates.

A thermal stimulator uses thermal energy to raise the reservoir temperature taking the composite hydrate molecule into a zone of instability. Thermal stimuli proposed in the literature are: (1) injection of hot fluids such as water, steam or brine, (2) combustion, and (3) electro-magnetic heating. *In situ* combustion relates to burning a portion of methane locally so that a flame front moves slowly from an injection well towards the production well. The gases released are at an elevated temperature and can be used directly for power generation. In option 3, microwaves or AC current heats up portions of the reservoir. Among the three methods of thermal stimulation for hydrate dissociation, fluid injection is well-developed and characterized in the laboratory. Further, it has been traditionally used as an enhancement technique for oil and gas recovery from conventional reservoirs.

Mathematical Modelling

Since experiments require a high-pressure environment in excess of 100 bar, numerical simulation continues to be the preferred method for research on gas recovery from hydrate reservoirs. The complexities of modelling and simulation are however quite overwhelming. The mathematical modelling of methane extraction involves multiphase transport, comprising phase-change and chemical reactions, in a moving-boundary system. Additional complexities include multiple length and timescales, media heterogeneity, and possible flow instabilities. Scarcity of experimental results also calls for molecular-scale modelling to derive the thermophysical properties, state equations, as well as the kinetics of the process. Numerical implementation of such models requires careful simplifications as well as suitably tailored algorithms. Extraction models available in the open literature ignore many such elements of complexity. On the other hand, highly accurate models are not available in the open literature. For an introduction, refer to the recent study of Khetan *et al*. (2013).

The success of modelling via a system of differential equations depends largely on the process parameters prescribed. Some of them include the permeability and dispersion tensors, interfacial transport coefficients, constitutive relations for capillary effects, and rates of reaction. Research on gas hydrates is new; references such as Moridis *et al*. (2009), White *et al*. (2011), Zatsepina *et al*. (2011), Fitzgerald *et al*. (2012) and Yuan *et al*. (2013) form a useful starting point. Accordingly, knowledge of parameters (and parametric functions) that will appear in the mathematical formulation is as yet incomplete. The expected values of these parameters must be determined from laboratory experiments. One strategy that can be used is to prepare gas hydrates on a laboratory scale and perform with it a recovery experiment. Laboratory-scale experiments can also be used to validate mathematical models of gas recovery.

Multi-phase Multi-component Model

A transient, non-isothermal, multiphase, multispecies model is presented here for the simulation of CH_4 gas production via depressurization and simultaneous CO_2 injection (Ahmadi *et al*., 2004; Sun *et al*., 2005; Uddin *et al*., 2008; Anderson *et al*., 2011; Khetan *et al*., 2013). The governing equations are written for simplicity in a one-dimensional Cartesian geometry bounded by the depressurization well at one end, and the injection well at the other. The present model accounts for transport phenomena in five phases, namely aqueous, gas, CH_4-hydrate, CO_2-hydrate, and the geological media. While the first two phases are mobile, the other three are treated as immobile. Such a distinction helps in accounting for the thermophysical properties of CH_4- and CO_2-hydrates. At a time instant and given location, all five phases present in the system are assumed to be in thermal equilibrium with each other. Temperature itself varies considerably over the spatial extent of the reservoir and is obtained as a part of the overall solution. The gas phase comprises a mixture of CH_4 and CO_2, while the aqueous phase contains only H_2O. The solubility of CH_4 and CO_2 gases in the aqueous phase and that of H_2O in the gas-phase can be shown to have negligible impact on gas recovery.

Experimental studies have shown that CO_2 hydrates are more stable than CH_4 hydrates only for temperatures below ~283.5 K. For pressures greater than the equilibrium pressure of CO_2 hydrate at 283.5 K, CO_2 gas starts to liquefy (Ota *et al*., 2005). Further, there is dearth of data for the kinetics of hydrate formation from liquid CO_2 and water. Hence, the present analysis is applicable to only that range of physical conditions where CO_2 remains either in gas- or in the hydrate-phase. The present model also neglects the effects of water salinity and turbidity as well as wettability and the pore size variation of the geological structure. Apart from methane recovery as a function of time, the model derives data for the distribution of pressure, temperature, and species concentration in the reservoir.

The following single step reactions describe the formation and decomposition of CH_4- and CO_2-hydrates:

$$CH_4(g) + N_h H_2O(l) \rightleftarrows CH_4.N_h H_2O(s) \quad (1)$$

$$CO_2(g) + N_h H_2O(l) \rightleftarrows CO_2.N_h H_2O(s) \quad (2)$$

Here, N_h, known as the hydration number, indicates the number of H_2O molecules required to encage each guest molecule. Mass conservation equations of CH_4, CO_2, and H_2O can be written by considering the mass of an individual species as the sum of species masses over all the phases. Hence

$$\phi \frac{\partial}{\partial t}\left(\rho_g s_g \omega_g^m + \rho_{mh} s_{mh} \omega_{mh}^m\right) = -\frac{\partial}{\partial x}\left(\rho_g \omega_g^m v_g + J_g^m\right) + \dot{m}_g^m + m_{mh}^m \quad (3)$$

$$\phi \frac{\partial}{\partial t}\left(\rho_g s_g \omega_g^c + \rho_{ch} s_{ch} \omega_{ch}^c\right) = -\frac{\partial}{\partial x}\left(\rho_g \omega_g^c v_g + J_g^c\right) + \dot{m}_g^c + m_{ch}^c \quad (4)$$

$$\phi \frac{\partial}{\partial t}\left(\rho_l s_l \omega_l^w + \rho_{mh} s_{mh} \omega_{mh}^w + \rho_{ch} s_{ch} \omega_{ch}^w\right) = -\frac{\partial}{\partial x}\left(\rho_l \omega_l^w v_l\right) + \dot{m}_l^w + m_{mh}^w + m_{ch}^w \quad (5)$$

Symbols appearing in the equations are described in the nomenclature. The velocity field is assumed to be Darcian and, therefore, the momentum conservation equation of each phase, in one-dimensional form, is expressed by:

$$v_\gamma = -\frac{K_{abs} k_{r\gamma}}{\mu_\gamma} \frac{\partial P_\gamma}{\partial x} \quad (6)$$

Using a volume averaged temperature over all the phases, thermal energy equation is written as:

$$\frac{\partial}{\partial t}\left[\sum_{\gamma=l,g,mh,ch}\left(\phi \rho_\gamma s_\gamma U_\gamma\right) + (1-\phi)\rho_s U_s\right] + \sum_{\gamma=l,g}\left[\sum_{i=m,c,w}\frac{\partial}{\partial x}\left(v_\gamma \rho_\gamma s_\gamma \omega_\gamma^i H_\gamma^i\right)\right] + \sum_{i=m,c}\frac{\partial}{\partial x}\left(J_g^i H_g^i\right) = \frac{\partial}{\partial x}\left(K_{eq}\frac{\partial T}{\partial x}\right) + \sum_{\gamma=l,g,mh,ch}\left[\sum_{i=m,c,w}\frac{\partial}{\partial x}\left(\dot{m}_\gamma^i H_\gamma^i\right)\right] + \dot{E} \quad (7)$$

The closure of the set of governing equations requires appropriate constitutive relations and reaction kinetics. The binary diffusive mass fluxes appearing in the gas-phase mass transport equations are expressed by Fick's law, namely:

$$J_g^i = -\phi\rho_g s_g D_g^i \frac{M^i}{M_g}\nabla(\chi_g^i) \tag{8}$$

The present study treats the liquid as incompressible and assumes ideal gas behaviour for the gas phase constituents (Eqs. 9-12). Mass fractions of various species in the hydrate phases are functions of the hydration number N_h and are determined using stoichiometric relations, Eqs. 13 and 14.

$$P_g = \rho_g \frac{R_u}{M_g} T \tag{9}$$

$$P_g = P_g^m + P_g^c \tag{10}$$

$$\chi_g^i = \frac{P_g^i}{P_g} \tag{11}$$

$$\omega_g^i = \frac{\rho_g^i}{\rho_g} \tag{12}$$

$$\omega_{ih}^i = \frac{M^i}{M^i + N_h M^w} \tag{13}$$

$$\omega_{ih}^w = \frac{N_h M^w}{M^i + N_h M^w} \tag{14}$$

Mass generation terms for the species considered in the model arise as a result of phase changes related to hydrate dissociation or formation. Consequently, when CH_4 hydrates dissociate, CH_4 mass generation in gas phase is positive, but in CH_4 hydrate phase it is equal and negative. Therefore, for any species *i*:

$$\sum_{\gamma=l,g,ch,mh} \dot{m}_\gamma^i = 0 \tag{15}$$

The kinetics of hydrate formation and dissociation are driven by independent interaction of CH_4 and CO_2 with liquid H_2O as well as the exchange of CO_2 and CH_4 within the H_2O-lattice. Recent experiments show that the exchange of CO_2 and CH_4 is usually negligible in class 3 reservoirs (Yuan *et al*. 2011). The rate of change of hydrate saturation (Eq. 16) can, therefore, be described by the Kim–Bishnoi kinetic model (Kim *et al*. 1987):

$$\phi\rho_{ih}\frac{\partial(s_{ih})}{\partial t} = \dot{m}_{ih} \tag{16}$$

$$\left[\dot{m}_{ih}\right]_f = \dot{m}_{ih} = M_{ih}(\phi A_{SH} s_l + \phi^2 A_{SH} s_l s_h)$$

$$K_f^i \exp\left(-\frac{E^i}{RT}\right)\left(P_g^i - P_{eq}^i\right) \tag{17}$$

$$s_h = s_{mh} + s_{ch} \tag{18}$$

$$\left[\dot{m}_{ih}\right]_d = -\dot{m}_{ih} = M_{ih}(\phi^2 A_{SH} s_l s_h)$$

$$K_d^i \exp\left(-\frac{E^i}{RT}\right)\left(P_{eq}^i - P_g^i\right) \tag{19}$$

The following three-phase equilibrium pressure data (MPa) of water-rich pure CH_4 and CO_2 hydrates, fitted to polynomial curves as a function of temperature (K) are adapted from Adisasmito *et al*., (1992):

$$P_{eq}^m = \left[0.1588\left(\frac{T-280.6}{4.447}\right)^3\right] + \left[0.6901\left(\frac{T-280.6}{4.447}\right)^2\right]$$

$$+\left[2.473\left(\frac{(T-280.6)}{4.447}\right)\right] + 5.513 \tag{20}$$

$$P_{eq}^c = \left[0.06539\left(\frac{(T-278.9)}{3.057}\right)^3\right] + \left[0.2738\left(\frac{(T-278.9)}{3.057}\right)^2\right]$$

$$+\left[0.9697\left(\frac{(T-278.9)}{3.057}\right)\right] + 2.479 \tag{21}$$

The above *P-T* relations may be modified by considering the effects of simultaneous presence of CH_4 and CO_2. Further experiments are, however, necessary to identify kinetic relations compatible with the improved thermodynamics.

The absolute permeability of the medium is a function of the effective fluid porosity ϕ_{lg}. An empirical relation between the two for Berea sandstone is given as:

$$K_{abs} = 5.51721(\phi_{lg})^{0.86} \times 10^{-15}\,\mathrm{m}^2, \phi_{lg} < 0.11$$

$$K_{abs} = 4.84653(\phi_{lg})^{0.86} \times 10^{-15}\,\mathrm{m}^2, \phi_{lg} \geq 0.11 \quad (22)$$

$$\phi_{lg} = (1 - s_h)\phi \quad (23)$$

Relative phase permeability functions (k_r) use the Corey model as:

$$k_{rl} = \left[\left(\frac{s_l}{s_l + s_g} - s_{lr}\right) \Big/ \left(1 - s_{lr} - s_{gr}\right)\right]^{n_l} \quad (24)$$

$$k_{rg} = \left[\left(\frac{s_g}{s_l + s_g} - s_{gr}\right) \Big/ \left(1 - s_{lr} - s_{gr}\right)\right]^{n_g} \quad (25)$$

The pressure difference between gas and the aqueous phase, known as the capillary pressure, is adapted from Sun *et al*. (2005) and written as:

$$P_c = P_g - P_w \quad (26)$$

$$P_c = P_{ec}\left[\left(\frac{s_l}{s_l + s_g} - s_{lr}\right) \Big/ \left(1 - s_{lr} - s_{gr}\right)\right]^{-n_c} \quad (27)$$

Here, P_{ec} is the entry capillary pressure and n_l, n_g and n_c are known constants. Water phase viscosity is assumed to be independent of pressure and temperature. Equations (28-34) for the gas phase viscosities and the mass diffusivities are adapted from the available correlations and are given as (Reid *et al*., 1987):

$$\mu_g = \frac{\chi_g^m \mu_g^m}{\chi_g^m + \chi_g^c \varphi_g^{cm}} + \frac{\chi_g^c \mu_g^c}{\chi_g^c + \chi_g^m \varphi_g^{mc}} \quad (28)$$

$$\varphi_g^{ij} = \left[1 + \left(\frac{\mu_g^i}{\mu_g^j}\right)^{1/2} \left(\frac{M^j}{M^i}\right)^{1/4}\right]^2 \left[8\left(1 + \frac{M^i}{M^j}\right)\right]^{-\frac{1}{2}} \quad (29)$$

$$D_g^{ij} = \frac{\left[3.03 - \left(\frac{0.98}{(M^{ij})^{1/2}}\right)\right]^2 T^{3/2}}{P_g (M^{ij})^{1/2} (\sigma^{ij})^2 \Omega_D} \times 10^{-2}\,\mathrm{m}^2/\mathrm{s} \quad (30)$$

$$M^{ij} = 2\left[\left(\frac{10^{-3}}{M^i}\right) + \left(\frac{10^{-3}}{M^j}\right)\right] \quad (31)$$

$$\sigma^{ij} = \frac{1.18(V_b^i)^{1/3} + 1.18(V_b^j)^{1/3}}{2} \quad (32)$$

$$T_r = \frac{T}{1.15\sqrt{T_b^i . T_b^j}} \quad (33)$$

$$\Omega_D = \frac{1.06036}{(T_r)^{0.1561}} + \frac{0.193}{\exp(0.47635 T_\gamma)} + \frac{1.03587}{\exp(1.52996T)} + \frac{1.76474}{\exp(3.89411 T_\gamma)} \quad (34)$$

Here V^i_b is the molar volume (cm^3/mol) at normal boiling point and T^i_b is the normal boiling point (K) for specie *i*. The specific heat capacities for the hydrate phases and solid rock medium are assumed to be invariant with respect to pressure and temperature. The specific heat capacities at constant pressure for CH_4 gas, CO_2 gas and water have been taken as functions of absolute temperature and are given as (Selim and Sloan, 1989):

$$C_{pg}^m = 1238.79 + (3.1303T) + (7.905 \times 10^{-4} T^2) - (6.858 \times 10^{-7} T^3)\ \mathrm{J/kg\text{-}K} \quad (35)$$

$$C_{pg}^c = 505.11 + (1.1411T) - (89.139 \times 10^{-5} T^2) + (210.566 \times 10^{-9} T^3)\ \mathrm{J/kg\text{-}K} \quad (36)$$

$$C_{pl}^w = 4023.976 + (0.57736T) - (8.314 \times 10^{-5} T^2)\ \mathrm{J/kg\text{-}K} \quad (37)$$

The heat source term occurring in the energy equation due to mass generation of species in different phases is modelled using the heat of hydrate formation. An energy balance provides the following thermodynamic relation for the energy source:

$$\sum_{\gamma = l,g,mh,ch} \sum_{i=m,c,w} \dot{m}_\gamma^i H_\gamma^i = \sum_{\gamma = g,mh} m_\gamma^m C_{p\gamma}^m T + \sum_{\gamma = g,ch} \dot{m}_\gamma^c C_{p\gamma}^c T + \sum_{\gamma = l,mh,ch} m_\gamma^w C_{p\gamma}^w T + \Delta H_{mh}^f(T)\, \dot{m}_{mh} + \Delta H_{ch}^f(T) m_{ch} \quad (38)$$

The enthalpies of reactions in which the gas hydrate dissociates into gas and water/ice can be determined by the direct use of the Clapeyron equation. The tabulated values for enthalpy were fitted to a polynomial curve as a function of temperature. The equations obtained are summarized below (Anderson *et al*., 2011):

The enthalpies of reactions in which the gas hydrate dissociates into gas and water/ice can be determined by the direct use of the Clapeyron equation. The tabulated values for enthalpy were fitted to a polynomial curve as a function of temperature. The equations obtained are summarized below (Anderson *et al*., 2011):

$$\Delta H^{f}_{mh}(T) = \left[30100.0\left(\frac{T-296.0}{14.42}\right)^{9}\right] - \left[12940.0\left(\frac{T-296.0}{14.42}\right)^{8}\right] - \left[160100.0\left(\frac{T-296.0}{14.42}\right)^{7}\right] + \left[69120.0\left(\frac{T-296.0}{14.42}\right)^{6}\right] + \left[285800.0\left(\frac{T-296.0}{14.42}\right)^{5}\right] - \left[119200.0\left(\frac{T-296.0}{14.42}\right)^{4}\right] - \left[193900.0\left(\frac{T-296.0}{14.42}\right)^{3}\right] + \left[68220.0\left(\frac{T-296.0}{14.42}\right)^{2}\right] + \left[37070.0\left(\frac{T-296.0}{14.42}\right)\right] + 420100.0\frac{J}{kg} \quad (39)$$

$$\Delta H^{f}_{ch}(T) = \left[2528.0\left(\frac{T-278.15}{2.739}\right)^{8}\right] + \left[75.36\left(\frac{T-278.15}{2.739}\right)^{7}\right] - \left[9727.0\left(\frac{T-278.15}{2.739}\right)^{6}\right] + \left[1125.0\left(\frac{T-278.15}{2.739}\right)^{5}\right] + \left[4000.0\left(\frac{T-278.15}{2.739}\right)^{4}\right] - \left[4154.0\left(\frac{T-278.15}{2.739}\right)^{3}\right] + \left[14430.0\left(\frac{T-278.15}{2.739}\right)^{2}\right] - \left[6668.0\left(\frac{T-278.15}{2.739}\right)\right] + 389900.0\frac{J}{kg} \quad (40)$$

Symbol $\dot{E}$, in the Eqn. (7) represents the external heat transfer rate due to longitudinal heat transfer from the over-burden and under-burden and is expressed as:

$$\dot{E} = \frac{P_{cs}}{A_{cs}}\Lambda(T_{init} - T) \quad (41)$$

The equivalent thermal conductivity in this analysis is calculated using a parallel mode of conduction and is given as:

$$K_{eq} = (1-\phi)K_s + \phi s_l K_l + \phi s_g K_g^m + \phi s_g K_g^c + \phi s_{mh} K_h^m + \phi s_{ch} K_h^c \quad (42)$$

Series mode of heat conduction is also possible in the reservoir and the equivalent thermal conductivity for such a case can be written as:

$$\frac{1}{K^s_{eq}} = \frac{\phi s_l}{K_l} + \frac{\phi s_g}{K_g^m} + \frac{\phi s_g}{K_g^c} + \frac{\phi s_{mh}}{K_{mh}} + \frac{\phi s_{ch}}{K_{ch}} + \frac{(1-\phi)}{K_s} \quad (43)$$

The present study, however, shows that the difference in the evolution of temperature is largely independent of the series or parallel models of thermal conductivity. Important parameters and constants that are used to close the above system of equations are adapted from Uddin *et al*. (2008) and summarized in Table 1.

Numerical Simulation

The model equations described above are numerically simulated for a class-3 reservoir bound above and below by impermeable rock layers as shown schematically in Fig. 2. The goal of the study is to understand the dynamics of simultaneous depressurization and CO_2 injection as well as to quantify the CO_2-hydrate and secondary CH_4-hydrate formation rates. There are two boundaries to the system: (1) production well (west boundary) and (2)

Table 1: Numerical values of the parameters used in the present simulation (Uddin *et al*., 2008)

Parameter, symbol	Value
Porosity, ϕ	0.28
CH_4 hydrate specific heat capacity, C_{pmh} (J/kg-K)	2220.0
CO_2 hydrate specific heat capacity, C_{pch} (J/kg-K)	2220.0
Solid rock specific heat capacity, C_{ps} (J/kg-K)	835.0
Aqueous thermal conductivity, K_l (W/m-K)	0.59
CH_4 gas thermal conductivity, K^m_g (W/m-K)	0.030
CO_2 gas thermal conductivity, K^c_g (W/m-K)	0.015
CH_4 hydrate thermal conductivity, K_{mh} (W/m-K)	0.62
CO_2 hydrate thermal conductivity, K_{ch} (W/m-K)	0.62
Rock thermal conductivity, K_s (W/m-K)	3.5
Irreducible aqueous phase saturation, s_{lr}	0.2
Irreducible gas phase saturation, s_{gr}	0.0
Hydration number, N_h	6.0
Aqueous phase density, ρ_l (kg/m^3)	1000.0
CH_4 hydrate phase density, ρ_{mh} (kg/m^3)	919.7
CO_2 hydrate phase density, ρ_{ch} (kg/m^3)	1100.0
Solid rock phase density, ρ_s (kg/m^3)	2675.08
CH_4 hydrate formation rate constant, K^m_f (mol/Pa-s-m^2)	0.00290
CH_4 hydrate dissociation rate constant, K^m_d (mol/Pa-s-m^2)	123960.0
CO_2 hydrate formation rate constant, K^c_f (mol/Pa-s-m^2)	0.00035
CO_2 hydrate dissociation rate constant, K^c_d (mol/Pa-s-m^2)	123960.0
CH_4 hydrate activation energy, E^m (J/mol)	81084.2
CO_2 hydrate activation energy, E^c (J/mol)	81084.2
Specific area of hydrates, A_{SH} (m^2/m^3)	375000.0
Aqueous phase viscosity, μ_l (Pa-s)	0.001
Pure CH_4 gas viscosity, μ^m_l (10^{-5} Pa-s)	1.35
Pure CO_2 gas viscosity, μ^c_l (10^{-5} Pa-s)	1.48
Entry capillary pressure, P_{ec} (Pa)	5000.0
Constant for aqueous relative permeability, n_l	4.0
Constant for gas relative permeability, n_g	2.0
Constant for capillary pressure, n_c	0.65
Longitudinal heat transfer constant, Λ (W/m^2-K)	1.0

injection well (east boundary). Initially, the reservoir core is partially saturated with CH_4 hydrate that is in equilibrium with water and free CH_4 gas. During operation, the production well is depressurized at a constant pressure, while CO_2 is injected simultaneously at a constant partial pressure at the injection well. At 283 K, CO_2 liquefies above ~4.5 MPa and the related kinetics of hydrate formation with liquid CO_2 is not well-understood. Hence, CO_2 injection pressure above 4.5 MPa and temperature above 283 K are not used in simulation. It is also assumed that the temperature always stays above the hydrate-gas-water-ice quadruple point so that no ice formation takes place. CH_4 gas production rate is defined as the rate (in kg/s) of CH_4 gas that flows out from the production well. Mathematically, the CH_4 gas production rate at the production well is calculated as:

$$\dot{M}^m_p = A_{CS}\omega^m_g \rho_g v_g\Big|_{west} \text{ kg/s} \tag{44}$$

Mass evolution rate of gaseous CH_4 in the reservoir is obtained by integrating the volumetric mass generation rate of CH_4 gas due to dissociation of CH_4 hydrates over the length of the entire reservoir as:

$$\dot{M}^m_e = -\left[\int_{x=0}^{x=L} \phi\omega^m_{mh}\rho_{mh}A_{CS}\frac{\partial(s_{mh})}{\partial t}dx\right] \text{kg/s} \tag{45}$$

Mass evolution rate signifies the extent to which hydrates dissociate to release gas. The gas production rate is directly proportional to the mass evolution rate. However, it must be noted that the reservoir considered in this study is not a closed system and the influx of CH_4 gas from the injection well, I^m into the reservoir adds to the production rate. Hence,

$$\dot{M}^m_p = M^m_e + \bar{I}^m \tag{46}$$

Initial and Boundary Conditions

To specify boundary conditions at each of the wells, we consider a realistic setting where several injection and production wells are laid out as a network of wells in a reservoir field. The pressure boundary condition at the production well is implemented on the total pressure rather than individual partial pressures of

the gas phase components. A Neumann boundary condition is enforced on the mass fractions of the gas components at the production well. Temperature is assumed to be distributed symmetrically around the production well and has a Neumann boundary condition. It is also possible to maintain a constant temperature at the production well by means of thermal stimulation, in which case a Dirichlet boundary condition is enforced.

The boundary condition for the total gas pressure at the injection well is difficult to specify as CO_2 gas is injected externally. For the present analysis, we assume that CO_2 is injected at such a flow rate such that its partial pressure at the injection well is always at a constant value of P^c_{inj}. Additionally, CH_4 gas partial pressure is assumed to be distributed symmetrically around the injection well and has a Neumann boundary condition. Consequently, the total gas pressure at the injection well is the sum of the CH_4 and CO_2 gas partial pressures. To take advantage of the sensible heat of injected CO_2 gas, a prescribed temperature is assigned at the injection well.

The initial and boundary conditions for the present simulations are given below.

Initial condition

$$P_g(x,0) = P_g^m(x,0) = P_{init};\ T(x,0) = T_{init};\ \omega_g^m(x,0) = 1.0$$
$$s_l(x,0) = s_{ol}; s_g(x,0) = s_{og};\ s_h(x,0) = s_{mh}(x,0) = s_{omh} \quad (47)$$

Boundary conditions

$$\frac{\partial[T(0,t)]}{\partial x} = 0;\ \frac{\partial[\omega_g^m(0,t)]}{\partial x} = \frac{\partial[\omega_g^c(0,t)]}{\partial x} = 0$$

At $x = 0$

$$\frac{\partial[s_g(0,t)]}{\partial x} = \frac{\partial[s_l(0,t)]}{\partial x} = 0; P_g(0,t) = P_{dep};\ P_c(0,t) = P_{ec} \quad (48)$$

At $x = L$

$$P_g^c(L,t) = P_{inj}^c; P_c(L,t) = P_{ec}; T(L,t) = T_{init}$$
$$\frac{\partial[P_g^m(L,t)]}{\partial x} = 0;\ \frac{\partial[s_g(L,t)]}{\partial x} = \frac{\partial[s_l(L,t)]}{\partial x} = 0 \quad (49)$$

Solution Procedure

The numerical solution of the governing equations uses a coupled, semi-implicit, iterative technique. The semi-implicit algorithm combines explicit kinetics with implicit transport in the following manner. The solution starts from the kinetic equation using the temperature and pressure from the previous time-step (Khetan *et al*., 2013). All other conservation equations are then solved implicitly. The temporal and spatial derivatives are discretized using forward- and central-differences, respectively while the Von Neumann and the Courant-Friedrichs-Levy stability criteria are enforced in the determination of the time step. Within each time-step, the convergence criterion, imposed by the iterative solver, ensures the evaluation of source-terms and transport parameters using the most recent values of the variables. Such a scheme resolves the nonlinear coupling among the equations.

Grid Independence and Validation

The numerical procedure developed for the present study was extensively scrutinized for grid size (Δx) and time-step size (Δt) independence. The effect of these numerical parameters was analysed on four primary system variables – total gas pressure, temperature, CH_4 hydrate saturation and CO_2 hydrate saturation. For the grid independence studies, the grid size was varied from Δx = 0.5 m to Δx = 4 m. The pressure values at the end of 30 days of simulation were within 1% of each other, being a maximum at the farthest point from the production well. Differences between grids with Δx = 0.5 and 1 m were negligible. Hence, a constant grid size of Δx = 1 m has been chosen for the final simulation.

The time step for the simulations was varied from Δt = 1.0 s to Δt = 12.0 s. The gas pressure profiles at the end of 30 days of production were practically invariant to the time-step. Hence, a time-step size of Δt = 10.0 s was chosen for the present simulations. In addition, incremental and cumulative balance checks for mass and energy contained in the reservoir were enforced at each time-step for ensuring accuracy of the solution. All simulation results, shown here, have been carried out with uniform Δx and constant Δt.

The simulation data were validated against the research of Sun *et al*. (2005) in terms of pressure and temperature distribution as a function of time. Results obtained from the present simulation show an excellent agreement. The maximum deviations between the two results are always less than 1%.

CO_2 Sequestration

Fig. 5 shows conditions under which CO_2 can form solid hydrates in the reservoir. Since methane release lowers temperature and CO_2 injection raises pressure, the conditions become increasing favourable for trapping CO_2 in the geological environment. Additional benefits of this approach include displacement of free methane gas and improvement in the structural strength of the reservoir, preventing it from collapse. This discussion is relevant in the context of a body of water, 1-2 km in depth, overlying the gas hydrate deposits.

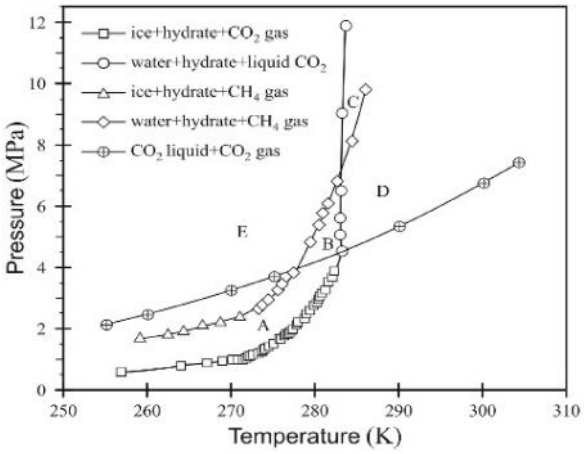

Fig. 5: Stability curves of methane and CO_2 hydrates shown jointly in the phase diagram. Since the stability boundary of CO_2 is below that of CH_4, it can act as a mobilizer of CH_4 while getting trapped in the reservoir as CO_2-hydrate. Hence, in regions marked A and B, methane is released as gas and CO_2 is trapped chemically as hydrate. Phase diagram of pure CO_2 is shown for comparison (adapted from Yuan *et al*., 2013)

Simulation Results

Simulation of the equations governing transport phenomena in a methane-hydrate reservoir contained between impermeable boundaries subjected to simultaneous depressurization and CO_2 injection has

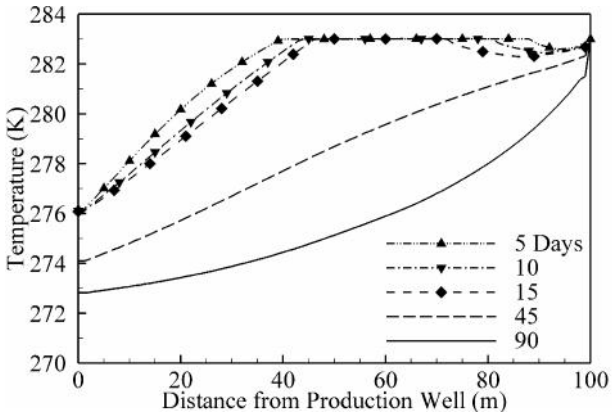

A

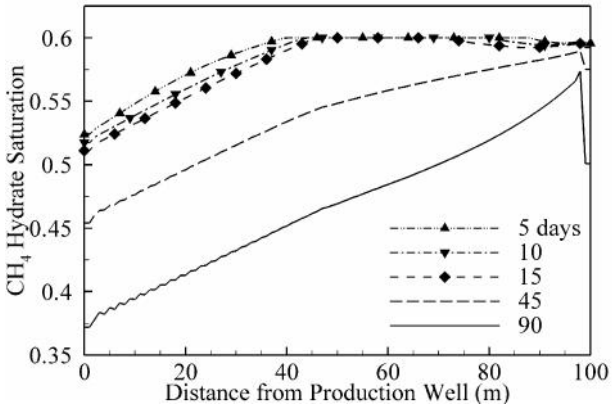

B

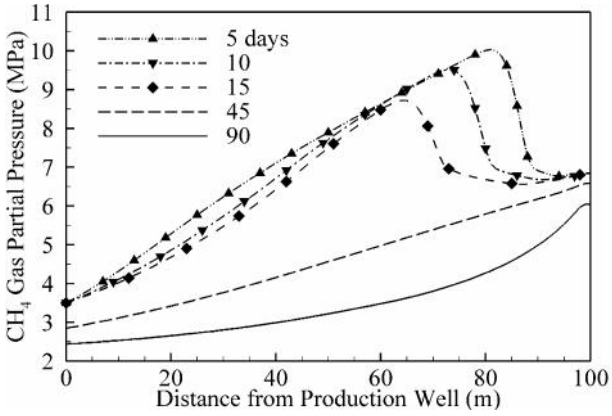

C

Fig. 6: A: Transient variation in the temperature of the hydrate reservoir subjected to simultaneous depressurization and CO_2 injection. Both depressurization and injection start at time t = 0. B: Transient variation in the CH_4 hydrate saturation within the 100 m hydrate reservoir subjected to simultaneous depressurization and injection and C: Transient variation of partial pressure of CH_4 within the reservoir subjected to depressurization and injection

been carried out. The model includes the unsteady, multi-phase, multispecies, non-isothermal transport and kinetics in a reservoir bounded between a depressurization and an injection well. Preliminary results of the study are summarized in Figs. 6 and 7. Since methane extraction from hydrate is an endothermic process, Fig. 6 shows the reservoir temperature progressively decreasing with time. Methane content of the reservoir diminishes with time while the gas partial pressure also decreases with time. The effect of process parameters on the overall gas recovered is presented in Fig. 7. As the depressurization pressure is lowered, the hydrates are further destabilized and additional methane is generated. Increasing the injection pressure of CO_2 displaces methane and gas recovery improves again. Fig. 7 also shows that the reservoir is emptied of methane while it gets filled with CO_2 in due course of time. Fig. 7 shows a rise in methane recovery several days into the operation of the wells of the reservoir. It corresponds to the time taken by the injected CO_2 at one end to mobilize methane towards the depressurization well.

Important conclusions relevant to the overall process are the following:

i. While CO_2 injection enhances CH_4 production, the enhancement is largely due to the displacement of CH_4. The CO_2-hydrate formation is a slow process and provides limited support for enhancement in CH_4-recovery. Slower kinetics and lower mole fractions restricts the CO_2-hydrate formation rate. While the production well pressure has minimal effect on the CO_2-hydrate formation, its saturation increases with increase in CO_2 injection pressure.

ii. CO_2 injection facilitates increases methane recovery, lowers reservoir temperature and can result in the formation of secondary CH_4-hydrates. The secondary hydrate formation is, however, quite small for the range of parameters studied. Secondary hydrate formation may also be lowered by lowering the production well pressure.

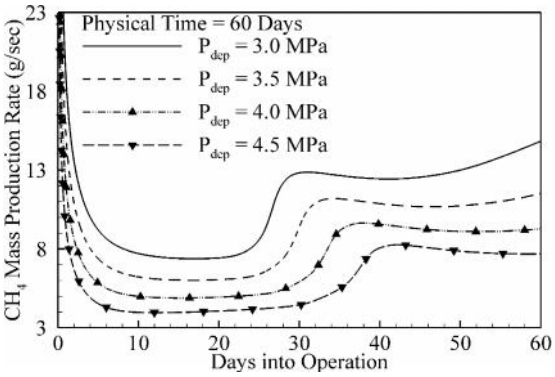

A

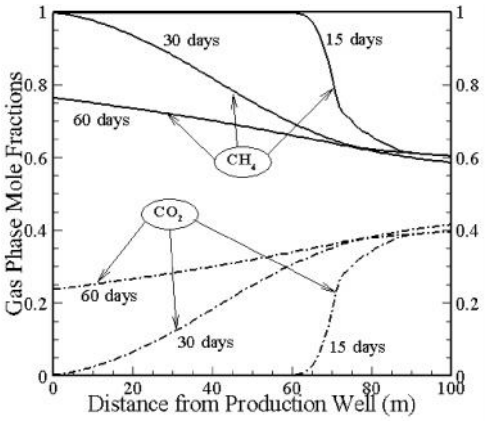

B

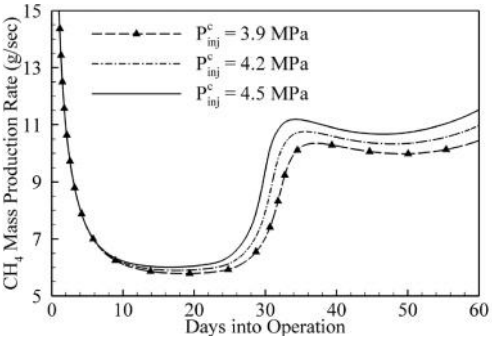

C

Fig. 7: A: Production rate of methane from a gas hydrate reservoir in which the left side is depressurized and the right side at a distance of 100 m has CO_2 injection. Reducing the depressurizing pressure from 4.5 to 3 MPa shows an increase in methane recovery rate, B: Amount of methane and CO_2 left in the reservoir after selected instants of time. The mobilities of the two gases are inter-related through chemical kinetics and because of the energy released and absorbed during hydrate formation and C: Influence of the CO_2 partial pressure at the injection well pressure on the mass production rate of CH_4 gas from the reservoir; CO_2-driven CH_4 increase in the mass evolution rate

iii. High rate of production may reduce the reservoir temperature leading to the solidification of H_2O. Such a phenomenon will reduce the reservoir-permeability gradually slowing down gas production. In this respect, the gas recovery process is self-limiting. The formation of CO_2 hydrates involves an exothermic reaction and has a beneficial effect on CH_4 recovery.

Further investigations, involving a three-dimensional geometry, phase-change effects and improved multiphase kinetics, are currently in progress.

Research Directions

Selection of an exploitation technique for gas recovery from hydrates calls for a fairly sophisticated analysis. Modelling the dissociation process itself for methane and formation process for CO_2 can proceed along two directions. The simpler direction is the *thermodynamic* approach utilizing Figures 3 and 4 in simulation. A realistic description would require a *kinetic* model involving rates of gas release or capture; such information can be derived only from laboratory experiments. Alternatively, a molecular-scale model for mixture thermodynamics and kinetics needs to be developed.

Flow distribution of methane along with the injected fluid, locally released gases, and moisture in a porous formation is a topic of research. Gas release depends on the distribution of pressure and temperature. The resulting model will involve multi-component, multiphase fluid flow, heat transfer, chemical reactions, and combustion in the subsurface. The fact that the pore structure of the reservoir is nowhere close to homogeneous is a point of concern. In this context, studies on imaging, reconstruction and characterization of the porous region are important. Data shows that pores display length scales over several orders of magnitude, calling for *multi-scale* modelling of the transport process in a stochastic framework. In addition, a reservoir experiencing fracture will alter the flow path, apart from the severe predicament of process safety.

Closure

Simultaneous exploitation of gas hydrates from its natural environ and disposal of CO_2 in its place is attractive but has considerable challenges, compelling a diversity of expertise. It calls for a need to examine and develop basic understanding of a complex interconnected system. Realizing the technology on a field scale will require across-the-board collaboration.

Nomenclature

A_{cs} Area of lateral heat transfer (m^2)

A_{SH} Specific area of hydrates (m^2)

C_p Specific heat capacity (J/kg-K)

D Mass diffusivity (m^2/s)

E Activation Energy (J)

H Enthalpy (J/kg)

$\bar{I}^m$ Methane influx (g/s)

J Mass flux (g/m^2-s)

K Thermal conductivity (W/m-K)

K_{eq} Equivalent thermal conductivity (W/m-K)

K_{abs} Absolute permeability

K_f Hydrate formation rate constant (mol/Pa-s-m^2)

K_d Hydrate dissociation rate constant (mol/Pa-s-m^2)

L Reservoir length (m)

M Molar mass (kg/kmol)

M^{ij} Function of molar masses of species i and j

$\dot{M}^m$ CH_4 production/evolution rate from the reservoir (kg/s)

$\dot{m}$ Mass generation rate at any x, t (kg/m^3-s)

N Hydration number

P Pressure (MPa)

R_u Universal gas constant (kg/kmol-K)

s Saturation

T Temperature (K)

t Time (s)

v Velocity (m/s)

x Horizontal co-ordinate axis

Greek Symbols

ϕ Porosity

ω Mass fraction

χ Mole fraction

μ Viscosity

ρ Density

Subscripts, Superscripts

c, ch CO_2, CO_2 hydrate

g, h, l Gas, hydrate, liquid

m, mh CH_4, CH_4 hydrate

p Production

w H_2O

γ Phases

References

Adisasmito S and Sloan E D (1992) Hydrates of carbon dioxide and methane mixtures *J Chem Eng Data* **37** 343-349

Ahmadi G, Ji C and Smith D H (2004) Numerical solution for natural gas production from methane hydrate dissociation *J Petrol Sci Eng* **41** 269-285

Anderson B J, Kurihara M, White M D, Moridis G J, Wilson S J, Pooladi-Darvish M, Gaddipati M, Masuda Y, Collett T S, Hunter R B, Narita H, Rose K and Boswell R (2011) Regional long-term production modeling from a single well test, Mount Elbert Gas Hydrate Stratigraphic Test Well, Alaska North Slope in *Mar Petrol Geol* **28** 493-501

Khetan, A, Das M K and Muralidhar K (2013) Analysis of methane production from a porous reservoir via simultaneous depressurization and CO_2 sequestration *Spec Top Rev Porous Media* **4** 237-252

Fitzgerald G C, Castaldi M J and Zhou Y (2012) Large scale reactor details and results for the formation and decomposition of methane hydrates via thermal stimulation dissociation *J Petrol Sci Eng* **94** 19-27

Kim H C, Bishnoi P R, Heidemann, R A and Rizvi S S H (1987) Kinetics of methane hydrate decomposition *Chem Eng Sci* **42** 1645-1653

Moridis G J, Collett T S, Boswell R, Kurihara M, Reagan M T and Koh C A (2009) Toward production from gas hydrates: current status, assesment of resources, and simulation-based evaluation of technology and potential *SPE Reserv Eval Eng* **12** 745-?71

Ota M, Morohashi K, Abe Y, Watanabe M, Smith-Jr R L and Inomata H (2005) Replacement of CH_4 in the hydrate using liquid CO_2 *Energ Conv Manage* **46** 1680-1691

Reid R C, Prausnitz J M and Poling B E (1987) The Properties of Gases and Liquids. New York, USA: McGraw-Hill Book Company

Sain K and Gupta H (2012) Gas hydrates in India: potential and development *Gond Res* **22** 645-657

Selim M S and Sloan Jr. E D (1989) Heat and mass transfer during the dissociation of hydrates in porous media *AIChE J* **35** 1049-1052

Sloan Jr. E D and Koh C A (2007) Clathrate Hydrates of Natural Gases 3rd Edition, Series: Chemical Industries, pp 119, CRC Press

Sun X, Nanchary N and Mohanty K K (2005) 1-D Modeling of hydrate depressurization in porous media *Transp Porous Media* **58** 315-338

Uddin M, Coombe D A, Law D and Gunter W D (2008) Numerical studies of gas *hydrate* formation and d**e**composition in a geological reservoir *ASME J Energ Resour Technol* **130** 10-17

White M D, Wurstner S K and McGrail B P (2011) Numerical studies of methane production from class 1 gas hydrate accumulations enhanced with carbon dioxide injection *Mar Petrol Geol* **28** 546-560

Yuan Q, Sun C-Y, Yang X, Ma P-C, Ma Z-W, i, Q-P and Chen G-J (2011) Gas production from methane-hydrate-bearing sands by ethanol glycol injection Using a three-dimensional reactor in *Energ Fuels* **25** 3108-3115

Yuan Q, Chang-Yu Sun, Bei Liu, Xue Wang, Zheng-Wei Ma, Qing-Lan Ma, Lan-Ying Yang, Guang-Jin Chen, Qing-Ping Li, Shi Li and Ke Zhang (2013) Methane recovery from natural gas hydrate in porous sediment using pressurized liquid CO_2 *Energ Conv Manage* **67** 257-264

Zatsepina O, Pooladi-Darvish M and Hong H (2011) Behavior of gas production from type (iii) hydrate reservoirs *J Nat Gas Sci Eng* **3** 496-504.